MaineDOT

Transportation Research Division

Technical Report 15-02

Bridge-in-a-Backpack™

Task 2.1 and 2.2: Investigate Alternative Shapes with Varying Radii

Final Report – February 2015

Technical Report Documentation Page

1. Report No. ME 15-02	2.	3. Recipient's Accession No.	
4. Title and Subtitle Bridge-in-a-Backpack™ Tasks 2.1 and 2.2: Investigating Alternative Shapes with Varying Radii – Computer Model Development and Shape Optimization		5. Report Date February 2015	
		6.	
7. Author(s) Keenan Goslin P.E. Xenia Rofes P.E.		8. Performing Organization Report No. AEWC Report Number 15-29-1023B	
9. Performing Organization Name and Address University of Maine – Advanced Structures and Composites Center		10. Project/Task/Work Unit No. Project 17891.00 – Tasks 2.1 & 2.2	
		11. Contract © or Grant (G) No. Contract # 20111223*2878	
12. Sponsoring Organization Name and Address Maine Department of Transportation		13. Type of Report and Period Covered	
		14. Sponsoring Agency Code	
15. Supplementary Notes			

16. Abstract (Limit 200 words)

This report includes fulfillment of Tasks 2.1 and 2.2 of a multi-task contract to further enhance concrete filled FRP tubes, or the Bridge in a Backpack. Task 2 is an investigation of alternative shapes for the FRP tubes with varying radii. Task 2.1 develops the computer model for FRP tubes with high gradients of fabric braid angle. Task 2.2 completes FRP tube shape optimization and laboratory testing of multi-radius arches.

UMaine has developed and licensed a hybrid composite arch bridge system. The main structural bridge elements utilize a tubular braided composite fabric that can be bent to a desired geometry. To date, only arches of constant radius have been fully analyzed, which sometimes pose a handicap due to clearance and/or hydraulic opening design requirements. This project uses the finite element code (FE Code) written by the University of Maine -Advanced Structures and Composites Center (The Center) developed in previous work (Clapp & Davids 2011, Clapp & Davids 2011) that takes into consideration soil-structure interaction amongst other things, and extends it to incorporate the effects unique to a multi-radius arch.

This project includes a parametric study, optimization of shapes and laboratory testing of multi-radius arches.

17. Document Analysis/Descriptors Arch bridges, concrete filled FRP tubes, construction, live load testing, Bridge-in-a-Backpack		18. Availability Statement	
19. Security Class (this report)	20. Security Class (this page)	21. No. of Pages 34	22. Price

THE UNIVERSITY OF MAINE

1865

ADVANCED STRUCTURES & composites center

Investigate Alternative Shapes with Varying Radii

Tasks 2.1 - Computer Model Development for Tubes

With High Gradients of Braid Angle

Task 2.2 –Shape Optimization and Laboratory Testing of

Multi-Radius Arches

Prepared for:

Dale Peabody P.E.
Director Transportation Research
Maine Dept. of Transportation
16 State House Station
Augusta, ME 04333-0016

University of Maine's Advanced Structures and Composites Center
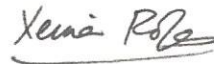**Report Number: 15-29-1023B**

February 15, 2015

Prepared by:

Keenan Goslin

Keenan Goslin P.E
Structural Engineer

Reviewed by:

Xenia Rofes

Xenia Rofes P.E.
Research Engineer

IAS

ACCREDITED

TABLE OF CONTENTS

UMaine Composites Center   Telephone: 207-581-2123
35 Flagstaff Rd   FAX: 207-581-2074
University of Maine   3   composites@umit.maine.edu
Orono, ME 04469   www.composites.umaine.edu

I. INTRODUCTION

UMaine has developed and licensed a hybrid composite arch bridge system. The main structural bridge elements utilize a tubular braided composite fabric that can be bent to a desired geometry. To date, only arches of constant radius have been fully analyzed, which sometimes pose a handicap due to clearance and/or hydraulic opening design requirements. This project uses the finite element code (FE Code) written by the University of Maine -Advanced Structures and Composites Center (The Center) developed in previous work (Clapp & Davids 2011, Clapp & Davids 2011) that takes into consideration soil-structure interaction amongst other things, and extends it to incorporate the effects unique to a multi-radius arch.

II. SUMMARY OF MODEL DEVELOPMENT

This document is intended to explore the effects of increasing the opening area of an arch by using multiple radii in the shape of the arch. Geometrically, arches of three different radii (i.e base or R_0, shoulder or R_s, and apex or R_a) have been considered for the analysis. Arches of this type can become a frame as the radii at the base and at the apex become large, and the shoulder radii are minimized.

Because the arch elements are made of tubular composite braid fabric, the tows (fibers) rearrange with different curvature, thus altering the strength and stiffness characteristics within the composite section. This non-linear effect has been incorporated in the FE code. As with current structural analysis software, all routines were written in MATLAB (MathWorks 2009) so that the user has full control over the analysis.

The following summarizes the main advances in the FE code through this project:

1. Generate an arch mesh routine by means of selecting a shoulder point and increasing its location outwardly. This results in an increased clear opening area as defined by the arch (i.e. hydraulic opening, *HO*)
2. Incorporate moment curvature relations for reinforced composite concrete sections as developed by Burgueno (Bannon 2009). This has two parts: A. calculation using Classical Lamination Theory and TsaiWu failure theory to predict laminate properties of the shell and B. Calculation of moment curvature relationships using Burgueno's method. A series of moment curvatures relations (M-phi plot) for a given radius of curvature 'Rc' are initially established for a series of axial loads and all radii used in the arch. The FE code uses interpolation for a given arch axial load to determine the corresponding element stiffness (slope in the M-phi plot) within the arch.

III. PARAMETRIC STUDY AND OPTIMIZATION

For this multi-radius study, a set of three bridge geometries for a given rise-to-span (R/S) ratio was selected. The minimum R/S considered was 0.3. Flatter arches are inherently inefficient due to high arch end moments, and thus not considered in this study.   The shoulder initial location for a given arch gets established about the original arch center point by an angle 'ϕ' from the horizontal. The shoulder point that allows the arch to become the most frame-like is defined by 'ϕo'such that:

$$\emptyset o = \operatorname{atan}\left(\frac{Ro}{0.5 * Span}\right)$$

where *Ro* is the original arch radius (constant). Arbitrarily, angles larger or smaller than 'ɸo'by 5 degrees have also been selected as options for the multi-arch study. A parameter 'η', defined as a percentage of how much can the shoulder stretch until it hits the arch apex height or span limit, is also varied in this study. Figure 1 shows the variables for the arch in comparison to a circular section.
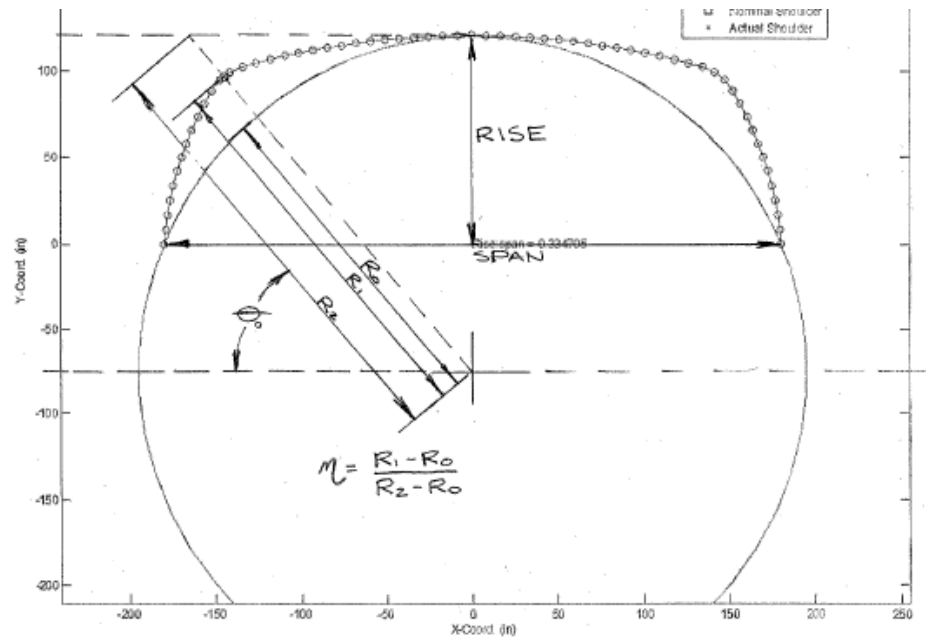
Figure 1 - Geometric Definitions

Table 1 shows the pertinent variables matrix selected for this study. Thus, a total of 30 different geometries are used for this parametric study, which correspond to:

- Three bridge types with R/S varying from 0.3, 0.35 and 0.4.
- Shoulder origin based on angle 'ɸ' ranging from ɸo-5 deg., ɸo, ɸo+5 deg.
- Shoulder increment parameter 'η' ranging from 0, 10, 20 and 30%. ('η' =0 corresponds to single radius arch)

Table 1 –Arch Geometry Matrix for Analyses

	φ (deg)	η (%)	Case Id	R₀ @ Base (ft)	Rₛ @ Shoulder (ft)	Rₐ @ −Apex (ft)	HO (%)
Rise/Span= 0.3			0	1	21.53	21.53	21.53	1.00
	φo - 5 deg.	10	2	35.93	11.54	24.87	1.01
		20	3	33.85	10.74	26.17	1.07
		30	4	47.64	8.45	27.18	1.12
	φo = 48.58 deg.	10	5	31.65	12.53	27.55	1.04
		20	6	41.05	6.67	30.26	1.10
		30	7	37.23	6.15	35.77	1.16
	φo+5 deg.	10	8	26.19	16.24	26.55	1.04
		20	9	31.84	10.87	30.67	1.07
		30	10	36.89	6.12	35.71	1.10
Rise/Span= 0.35			0	11	20.22	20.22	20.22	1.00
	φo - 5 deg.	10	12	34.69	12.06	23.06	1.02
		20	13	40.69	9.47	24.56	1.07
		30	14	37.94	9.21	25.65	1.13
	φo = 46.79 deg.	10	15	32.82	10.47	25.93	1.03
		20	16	32.40	7.74	29.04	1.09
		30	17	33.79	6.03	33.43	1.15
	φo + 5 deg.	10	18	28.20	14.40	24.70	1.03
		20	19	28.63	10.70	27.48	1.07
		30	20	32.53	6.00	34.33	1.09
Rise/Span= 0.4			0	21	19.48	19.48	19.48	1.00
	φo - 5 deg.	10	22	33.69	10.60	23.06	1.03
		20	23	40.92	8.06	26.39	1.08
		30	24	30.92	10.00	32.35	1.15
	φo = 45.72 deg.	10	25	28.65	12.37	24.89	1.03
		20	26	28.95	9.66	28.32	1.09
		30	27	27.89	7.39	37.08	1.13
	φo + 5 deg.	10	28	28.32	14.35	24.27	1.03
		20	29	25.94	10.09	28.19	1.06
		30	30	32.42	6.00	32.84	1.08

Note that for each of the selections, the maximum hydraulic opening attained is in the order of 15% to 16% increase (*HO*=1.16) which corresponds to Cases Id #7, #17 and #30.

For the analysis, the structures were analyzed with a concrete topped deck present and its stiffness incorporated in the analysis in both the longitudinal and transverse direction. Soil springs were included throughout the arch elements to simulate arch soil interaction. The bridges where founded on a 4' high x 4 ft wide continuous spread footing with a base friction coefficient of 0.6 typically used in conventional foundation design, since this foundation proved to be sufficient to prevent footing lateral movement for all loading conditions. In addition, earth backfilling affects based on 24 in lifts applied to alternating sides of the arch were also included

UMaine Composites Center
35 Flagstaff Rd
University of Maine
Orono, ME 04469

6

Telephone: 207-581-2123
FAX: 207-581-2074
composites@umit.maine.edu
www.composites.umaine.edu

in the model. The following design parameters (Table 2) were set constant for the parametric study:

Table 2 – Specific Parameter Values for Analyses

Description	FE Code Variable	Units	Value
Diameter of CFRP tube	diam	in	11.6
Span of arch centerline	span	ft	38
Depth of backfill above arch crown	depth_crown	ft	4
Arch spacing	spacing	ft	3
Design truck axle	Axle_space	-	Short (14')
Number of lanes loaded	num_lanes	-	2

ARCH CONSTITUTIVE RELATIONS

Although commercially there have been a combination and carbon outer layer and glass inner layer for their composite tubes, recent designs have used an all glass tube in bridge design, providing several benefits that include:

1. Increase in wall thickness which translates to greater buckling resistance during filling and greater in-situ abrasion resistance
2. Increase in shear resistance
3. Increase in braid jam angle which translates to smaller manufacturing bent radii.

It is mainly for the above reasons that, for this study, a one-inner-and-three-outer layer glass tube was used for the arch elements with the following micro-mechanic parameters (Table 3).

Table 3 - Micro-mechanics properties of FRP tubes

Braid Characteristic	Confinement-Hybon 2022 Roving 250	Structural-Hybon 2022 Roving 250
Outer Diameter (in)	11.6	11.6
Nominal braid Angle °	75	22
Raw Fiber Yield (yd/lb)	250	250
Fiber Density (lb/in^3)	0.092	0.092
Fiber Volume	**50%**	**50%**
Layer Thickness (in)	**0.039**	**0.0569**
Number of Layers	**1**	**3**

The resulting total tube thickness was estimated at 0.2096 in., with the Structural Glass laminate thickness (3 layers) being 0.1707 inches.

UMaine Composites Center
35 Flagstaff Rd
University of Maine
Orono, ME 04469

7

Telephone: 207-581-2123
FAX: 207-581-2074
composites@umit.maine.edu
www.composites.umaine.edu

It is to note that, when comparing the mechanical properties for this all glass tube to the original carbon tube in the first bridge application (Bannon 2009), the moment capacity was calculated in the range of 95 to 100% that of carbon, whereas the shear capacity was calculated in the range of 150% to 160% that of carbon.

The minimum radius of curvature at the arch centerline for a 22degree braid angle and a 11.6-in. outer diameter tube was calculated at about 74 inches, and for this analysis it was rounded up to 80 inches to potentially exclude wrinking effects and other manufacturing limitations of such tight radii.

Some simplifications were made to select braid properties in the FE Code when generating a multi-radius arch. For radius less than 100 in., the selected radius of curvature R_c values were rounded to the nearest tens. For radii greater than 100 in., they were rounded to the nearest 100s (i.e. radius of 80, 90, 100, 200, etc…). Within this parametric study, the maximum R_c value considered was 600 inches.

The braid angle of the tubes changes along the cross section when the tubes are bent to forming an arch. The tube thickness also varies with braid angle, implying that the cross section wall has varying thickness, with thinnest wall section at the top of the tube (where transverse decking is connected), and thickest wall section at the bottom of the tube (where braid angle is the least). The range of braid angle, also referred to as 'bias', and equivalent top and bottom tube thickness are presented in Table 4 for a given set of radius of curvature, Rc. Numerical algorithms are used to estimate the circumferential cross sectional area based on a prescribed number of segments (100 minimum). Stresses, and thus moment capacity, are then computed for each arch element.

Table 4 – Ranges of braid angle for a given Rc

Rc (in)	Min braid angle (deg.)	Max. braid angle (deg.)	Min. FRP thickness (in)	Max FRP thickness (in)
80	7.02	30.44	0.1595	0.1835
100	11.64	28.94	0.1616	0.1810
300	19.07	24.55	0.1675	0.1740
600	20.62	23.29	0.1692	0.1723
Inf	22.00	22.00	0.1707	0.1707

UMaine Composites Center
35 Flagstaff Rd
University of Maine
Orono, ME 04469

8

Telephone: 207-581-2123
FAX: 207-581-2074
composites@umit.maine.edu
www.composites.umaine.edu

The following were the resulting mechanical properties estimated for the laminate (Rc = Inf):

- Ex=3700 ksi & Fxt=21 ksi stiffness and ultimate strength in longitudinal direction
- Ey=2000 ksi & Fyt= 11 ksi stiffness and ultimate strength in transverse direction
- eut=0.0058 in/in ultimate strain at 0 axial load in longitudinal direction
- euh=0.006 in/in ultimate strain at 0 axial load in transverse (hoop) direction
- vxy=0.44 poisson's ratio

These values are more conservative than those found at the Center in previous coupon tests (Bannon 2009) and currently used by Advanced Infrastructure Technologies (AIT) in their capacity spreadsheet. Ultimate failure values have been conservatively estimated using Tsai-Wu failure theory. However, the ultimate curvature from the M-phi curves has not been implemented as an arch failure criterion in the final multi-radius FE model, but rather used as a tool to estimate element stiffness degradation with increasing axial load and is thus considered valid for this study.

The following curves in Figure 2 exemplify the non-linear M-phi relations with applied axial loads for a tight radius of curvature (Rc=80 in.) versus a larger one (Rc=600 in.). The main difference between the plots is that there is an increase in stiffness for positive moment (tension at bottom) by increasing bend radius. The opposite takes place for the negative moment. Curvature increases with axial load as expected.

The negative moment capacity is slightly greater than the positive moment capacity suggesting that the change in braid angle has a larger effect that the change in section thickness.

UMaine Composites Center
35 Flagstaff Rd
University of Maine
Orono, ME 04469

9

Telephone: 207-581-2123
FAX: 207-581-2074
composites@umit.maine.edu
www.composites.umaine.edu
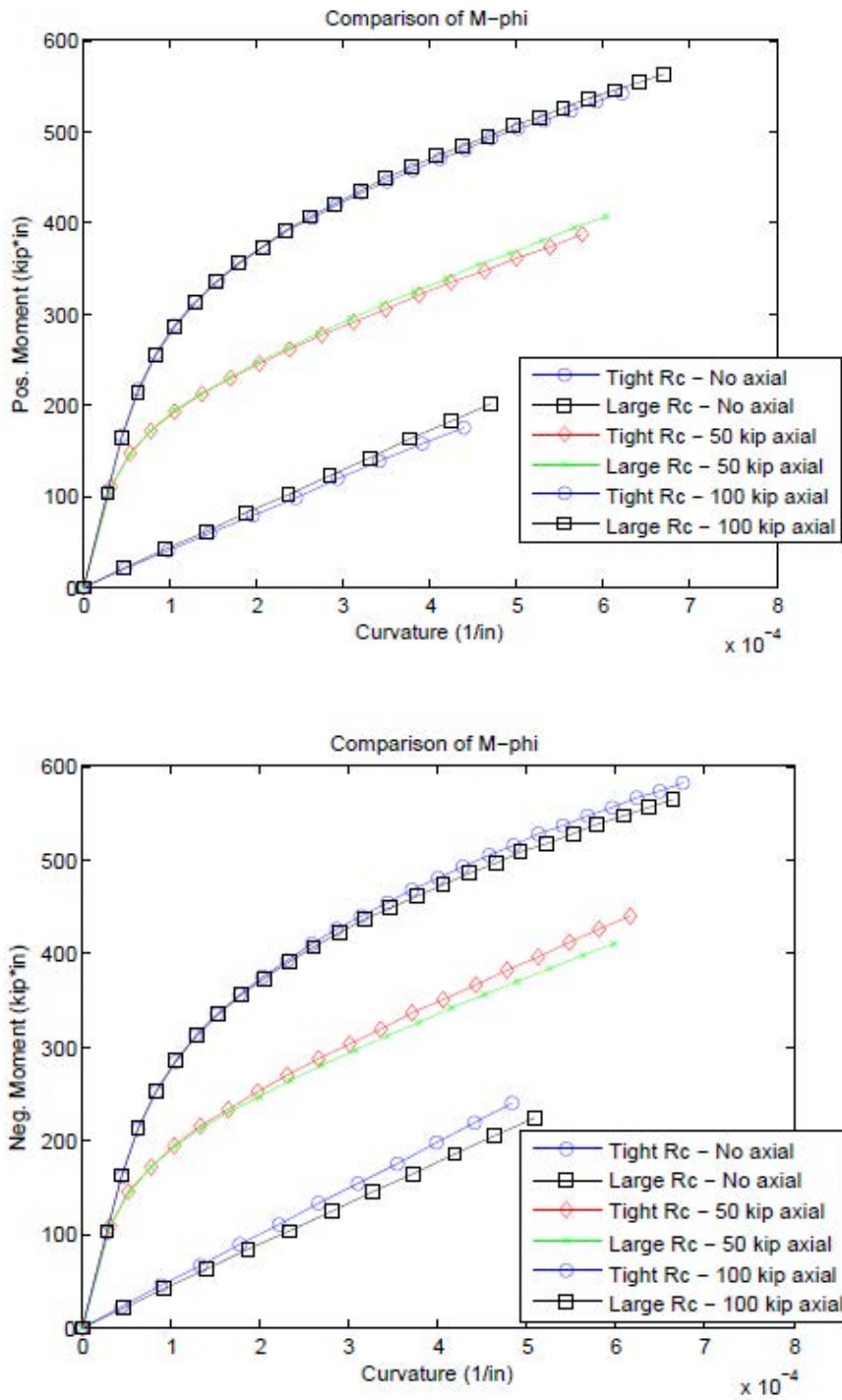
Figure 2- Comparison of Positive and Negative M-phi relation for a Tight (80") and Large (600") Rc

RESULTS AND DISCUSSION

ARCH FORCE EFFECTS:

Key results are summarized in Table 5 and Table 6 for the 30 cases analyzed (refer to Table 1 for parametric study Case multi-radius arch geometry). Note that M_ratio, P_ratio and V_ratio are

UMaine Composites Center
35 Flagstaff Rd
University of Maine
Orono, ME 04469

10

Telephone: 207-581-2123
FAX: 207-581-2074
composites@umit.maine.edu
www.composites.umaine.edu

the ratios of the moment, axial and shear arch effects relative to the arch with 'η' of zero for the same R/S ratio, so that run Case #17 with M_ratio of 2.0 undergoes twice the moment than if the same arch was not multi-radius (run Case #11). M_control is the controlling moment at the base of the multi-radius arch, or along the arch itself, and if it is positive or negative (i.e. 'int+' implies positive moment along the arch controls).

It is apparent that making the arch a multi-radius arch has a detrimental effect on the arch design, increasing the maximum internal factored moment 'Mu' in the arch, while increasing the factored shear load, 'Vu'. In a general sense, the smaller the curvature at the shoulder (or the larger'η'is), the worse the effect. Furthermore, as the R/S ratio increases, the detrimental shear effect decreases, although the arch moment effect increases.

The change in minimum axial load, 'Pu', as can be seen in Table 4, remains fairly constant and it is thus not a variable for discussion in this study.

It is worth noting the moment reversal within the arch in this parametric study (refer to Figure 3 for sign convention). At R/S=0.30 and 0.35, the governing moment for the single radius arch is at the base in negative bending (run Cases #1 and #11). Then, for low angle'ϕ'(initial shoulder angle from horizontal closest to foundation) and low 'η's, there is a base moment reversal so that a positive moment governs at the base. Thereafter, internal moments are the governing ones. Generally speaking, positive bending governs at around the crown or at the apex, and negative moments occur at the shoulders. The exception is for run Case #22 with R/S=0.4, where the governing moment is a positive internal moment at the shoulder.
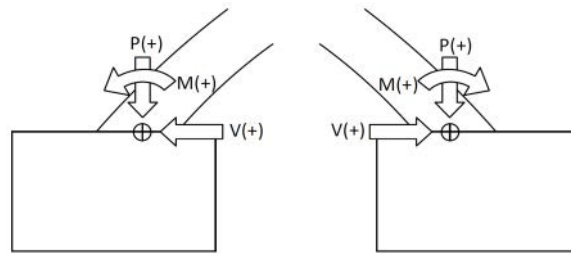
Figure 3 - Schematic of Sign Convention

For a single radius arch, as the rise increases, the radius of curvature of the arch decreases, and the thrust at the base decreases due to the lateral earth restraining capability. This causes the negative arch moment to decrease at the base and thus making the positive apex moment the governing one. This can be seen for run Case #21.

For ϕ greater than or equal to ϕo, as 'η' is set to 30% so that the arch is more "frame-like", the governing moment is always at the shoulder in negative bending.

UMaine Composites Center
35 Flagstaff Rd
University of Maine   11
Orono, ME 04469

Telephone: 207-581-2123
FAX: 207-581-2074
composites@umit.maine.edu
www.composites.umaine.edu

Table 5 - Summary of Factored (Strength I) Arch Forces

	Run ID	Max. Mu (kip-in)	Min. Pu (kip)	Max. Pu (kip)	Max Vu (kips)	M_ ratio	P_ ratio	V_ ratio	M_ control
Rise/Span= 0.3	1	-364.2	16.6	52.5	7.3	1.0	1.0	1.0	base -
	2	360.6	19.8	50.8	12.8	1.0	1.2	1.8	base+
	3	397.1	19.0	49.0	13.2	1.1	1.1	1.8	base+
	4	-411.2	17.9	46.0	14.9	1.1	1.1	2.0	int-
	5	344.5	18.4	48.0	9.9	0.9	1.1	1.4	int+
	6	-518.6	18.9	48.3	17.3	1.4	1.1	2.4	int-
	7	-694.5	18.6	49.1	21.6	1.9	1.1	3.0	int-
	8	302.3	17.0	44.6	7.6	0.8	1.0	1.0	int+
	9	418.7	17.1	46.7	12.0	1.1	1.0	1.6	int-
	10	-665.8	18.3	48.3	20.3	1.8	1.1	2.8	int-
Rise/Span= 0.35	11	-324.7	15.9	51.5	7.6	1.0	1.0	1.0	base -
	12	317.1	17.4	50.2	9.3	1.0	1.1	1.2	base+
	13	-349.5	17.7	43.4	11.2	1.1	1.1	1.5	int-
	14	-379.8	16.4	42.4	12.2	1.2	1.0	1.6	int-
	15	344.6	18.1	46.5	10.6	1.1	1.1	1.4	int+
	16	-482.7	18.1	45.9	14.4	1.5	1.1	1.9	int-
	17	-663.5	17.7	47.0	19.9	2.0	1.1	2.6	int-
	18	310.4	16.5	42.7	7.1	1.0	1.0	0.9	int+
	19	384.3	15.7	43.1	10.5	1.2	1.0	1.4	int+
	20	-657.4	17.8	46.7	19.7	2.0	1.1	2.6	int-
Rise/Span= 0.4	21	313.8	15.4	39.2	10.1	1.0	1.0	1.0	int+
	22	334.7	17.2	44.0	10.2	1.1	1.1	1.0	int+
	23	-427.4	17.5	43.6	13.1	1.4	1.1	1.3	int-
	24	530.6	17.7	49.8	13.6	1.7	1.1	1.3	int+
	25	344.7	17.3	44.6	8.7	1.1	1.1	0.9	int+
	26	425.1	16.8	45.9	12.0	1.4	1.1	1.2	int+
	27	-727.6	19.1	50.0	17.6	2.3	1.2	1.7	int-
	28	318.1	16.4	42.1	7.1	1.0	1.1	0.7	int+
	29	408.5	16.4	44.1	11.1	1.3	1.1	1.1	int+
	30	-631.4	17.1	44.9	18.9	2.0	1.1	1.9	int-

FOUNDATION EFFECTS:

The arch was modeled with a 4 ft wide by 4 ft high continuous spread foundation. That was sufficient to prevent all arches from moving laterally. The arches behaved as with arches with fixed-ends, which is what is currently designed by AIT. The reaction effects in this parametric study are shown in Table 6 for service load conditions in terms of moment (Ms), axial load (Ps) and shear (Vs). It is clear that, unlike for single radius arches, the governing foundation moment is in the positive direction (refer to Figure 3). As 'η'increases, the positive moment increases for a given 'φ'to the point that it can exceed the negative moment of the initial single radius arch. This is stated by an M_ratio>1.0 (i.e. run Case #7).

UMaine Composites Center
35 Flagstaff Rd
University of Maine
Orono, ME 04469

12

Telephone: 207-581-2123
FAX: 207-581-2074
composites@umit.maine.edu
www.composites.umaine.edu

A multi-radius arch simplifies arch foundation since it only needs to be designed for moments in one direction in many cases (i.e. for $\phi < \phi_o$ +5 deg). Since the outward thrust causes the foundation to rotate in the same direction as the positive moment, the effect of the two are cumulative. Due to the fact that bridge foundations over water passages are often designed to large depths to prevent frost and/or scour, the outward thrust is always the governing force in foundation design, and since it is less for all multi-radius arches, foundations should ultimately become more cost effective for this type of structures.

DEFLECTION EFFECTS

Deflection effects in this study are summarized in Table 7 for both positive (upward) and negative (downward) deflections. Positive deflections occur near the shoulders and negative deflections are worst at or near the arch apex. A simplification on this study has been made to attempt to isolate the deflection due to lane and truck alone, so as to estimate a deflection trend, understanding that the nature of this non-linear analysis makes such values not realistic.

Note that dead load deflections alone can be substantial for multi-radius arches, especially with an increase of R/S, and that often the dead load deflection makes up for more than half the total deflection in the arch, which is typical of buried structures.

Both upward and downward deflection increases with an increase in 'η'. Total deflections are worst for $\phi = \phi_o$ where "frame-like" structures are maximized. As R/S increases, the deflection experienced by the arches also increases. Based on this model, a R/S of 0.4 or greater behaves poorly because of deflection, and should be considered an upper bond for multi-radius arches unless 'η'< 10%.

Based on the high deflections experienced within this parametric study, one can conclude that the three structural layer glass tube with properties as discussed in the previous section might not offer enough stiffness for many multi-radius arch geometries.

UMaine Composites Center
35 Flagstaff Rd
University of Maine   13
Orono, ME 04469

Telephone: 207-581-2123
FAX: 207-581-2074
composites@umit.maine.edu
www.composites.umaine.edu

Table 6 – Summary of Service Reaction

	Run ID	Max Ms (kip-in)	Max Ps (kip)	Max Vs (kips)	M_ ratio	P_ ratio	V_ ratio
	1	-236.8	71.0	39.9	1.0	1.0	1.0
	2	258.4	68.9	35.7	1.1	0.9	0.9
0.3	3	289.0	67.7	31.6	1.2	0.9	0.8
	4	298.8	65.6	25.5	1.3	0.8	0.6
	5	215.7	68.8	34.6	0.9	0.9	0.9
	6	212.2	66.2	26.6	0.9	0.8	0.7
Rise/Span=	7	252.5	63.3	18.4	1.1	0.7	0.5
	8	154.6	68.8	37.0	0.7	0.9	0.9
	9	154.3	67.1	31.8	0.7	0.9	0.8
	10	145.2	65.8	26.6	0.6	0.8	0.7
	11	-204.6	74.1	31.3	1.0	1.0	1.0
	12	192.2	72.4	28.6	0.9	0.9	0.9
0.35	13	214.2	70.1	22.9	1.0	0.9	0.7
	14	240.4	67.5	18.5	1.2	0.8	0.6
	15	168.1	72.0	26.8	0.8	0.9	0.9
	16	190.5	68.5	19.7	0.9	0.8	0.6
Rise/Span=	17	200.7	65.4	13.5	1.0	0.7	0.4
	18	-144.4	71.9	28.5	0.7	0.9	0.9
	19	139.6	69.0	24.0	0.7	0.9	0.8
	20	129.7	68.4	20.2	0.6	0.8	0.6
	21	-142.1	76.7	24.4	1.0	1.0	1.0
	22	186.7	74.0	19.2	1.3	0.9	0.8
0.4	23	202.1	70.7	12.7	1.4	0.8	0.5
	24	305.0	66.2	5.8	2.1	0.7	0.2
	25	187.9	73.9	19.7	1.3	0.9	0.8
	26	204.1	70.1	13.7	1.4	0.9	0.6
Rise/Span=	27	227.7	67.6	8.1	1.6	0.8	0.3
	28	-168.5	74.4	20.9	1.2	1.0	0.9
	29	164.3	72.1	17.7	1.2	0.9	0.7
	30	95.1	70.5	14.3	0.7	0.9	0.6

UMaine Composites Center
35 Flagstaff Rd
University of Maine
Orono, ME 04469
14
Telephone: 207-581-2123
FAX: 207-581-2074
composites@umit.maine.edu
www.composites.umaine.edu

Table 7 - Summary of Maximum Deflections (inches)

	Run ID	Upward Deflection (positive)					Downward Deflection (negative)				
		DL	DL+E+WS	LL_lane	LL_truck	TOTAL	DL	DL+E+WS	LL_lane	LL_truck	TOTAL
0.3 ... **Rise/Span=**	1	0.068	0.373	0.007	0.188	**0.568**	-0.136	-0.293	-0.002	-0.150	**-0.445**
	2	0.177	0.080	0.008	0.112	**0.199**	-0.409	-0.269	0.000	-0.353	**-0.622**
	3	0.231	0.141	0.007	0.141	**0.289**	-0.559	-0.383	0.000	-0.456	**-0.839**
	4	0.307	0.239	0.008	0.183	**0.430**	-0.774	-0.580	0.001	-0.629	**-1.209**
	5	0.207	0.123	0.000	0.175	**0.298**	-0.543	-0.368	0.001	-0.573	**-0.941**
	6	0.323	0.282	0.028	0.313	**0.622**	-0.944	-0.957	0.002	-0.996	**-1.953**
	7	0.455	0.536	0.047	0.481	1.064	-1.560	-2.091	-0.030	-1.741	-3.862
	8	0.151	0.075	0.000	0.223	**0.298**	-0.376	-0.135	0.000	-0.422	**-0.557**
	9	0.234	0.184	0.000	0.216	**0.400**	-0.688	-0.567	-0.001	-0.918	**-1.486**
	10	0.305	0.309	0.040	0.434	**0.783**	-1.060	-1.480	-0.024	-1.505	**-3.010**
0.35 ... **Rise/Span=**	11	0.129	0.524	0.017	0.228	**0.769**	-0.232	-0.398	-0.028	-0.210	**-0.636**
	12	0.264	0.062	0.009	0.148	**0.219**	-0.551	-0.227	-0.051	-0.420	**-0.697**
	13	0.367	0.161	0.013	0.150	**0.324**	-0.822	-0.382	-0.068	-0.542	**-0.991**
	14	0.465	0.255	0.016	0.172	**0.443**	-1.080	-0.544	-0.078	-0.688	**-1.310**
	15	0.312	0.126	0.019	0.163	**0.308**	-0.755	-0.377	-0.058	-0.629	**-1.064**
	16	0.449	0.286	0.024	0.307	**0.617**	-1.215	-0.941	-0.072	-1.073	**-2.086**
	17	0.599	0.529	0.038	0.456	**1.023**	-1.851	-1.911	-0.125	-1.726	**-3.762**
	18	0.230	0.092	0.032	0.221	**0.345**	-0.519	-0.134	-0.030	-0.402	**-0.567**
	19	0.320	0.129	0.029	0.212	**0.370**	-0.812	-0.312	-0.061	-0.886	**-1.259**
	20	0.409	0.279	0.035	0.445	**0.759**	-1.299	-1.405	-0.121	-1.626	**-3.153**
0.4 ... **Rise/Span=**	21	0.229	1.106	-0.440	-0.256	**1.106**	-0.385	-0.792	0.269	0.080	**-0.792**
	22	0.455	0.239	-0.131	-0.011	**0.293**	-0.940	-0.268	-0.155	-0.597	**-1.019**
	23	0.662	0.158	0.238	0.424	**0.820**	-1.576	-0.501	-0.509	-1.274	**-2.285**
	24	0.899	0.391	0.271	0.552	**1.214**	-2.467	-1.134	-0.912	-2.378	**-4.423**
	25	0.440	0.184	-0.053	0.094	**0.225**	-0.971	-0.238	-0.145	-0.691	**-1.074**
	26	0.612	0.109	0.132	0.406	**0.647**	-1.522	-0.296	-0.629	-1.645	**-2.571**
	27	0.810	0.367	0.334	0.790	**1.491**	-2.513	-1.585	-1.362	-3.318	**-6.265**
	28	0.342	0.555	-0.339	-0.149	**0.555**	-0.717	-0.431	0.161	-0.109	**-0.540**
	29	0.460	0.165	0.039	0.225	**0.429**	-1.127	-0.220	-0.282	-1.247	**-1.748**
	30	0.532	0.182	0.135	0.476	**0.793**	-1.528	-0.373	-1.041	-2.534	**-3.948**

COST EVALUATION - CASE STUDY

It is apparent that a multi-radius arch will incur additional cost due to the increase of its internal moments; However, the reduction in foundation thrust will make its foundation smaller, thus resulting in potential savings that would offset the arch cost. In this section, the multi-radius arch represented in Case #17 ($\phi = \phi_o$, 'η'< 30%) is compared with its equivalent single radius represented in Case #11 (span of 38 ft, rise of 13.3 ft, and radius of 20.22 ft) in terms of foundation, deck and arch member potential costs. Table 8 summarizes the pertinent values of output values from the FE analysis as follows:

UMaine Composites Center
35 Flagstaff Rd
University of Maine
Orono, ME 04469

15

Telephone: 207-581-2123
FAX: 207-581-2074
composites@umit.maine.edu
www.composites.umaine.edu

Table 8 – Summary of Output Results for multi-radius arch of Case #17

R/S	φ (deg)	Type	M_ratio	P_ratio	V_ratio	Δ_ratio + (up)	Δ_ratio – (down)
0.35	46.79	Arch –	2.04[1]	1.12[1]	2.61[1]	1.33[2]	5.91[2]
		Fdn -	0.98[2]	0.75[2]	0.43[2]	na	na

(1)Strength I values; (2) Service values

When calculating the structure foundations, the following assumptions have been made.

1. Angle of soil friction = 35 degrees
2. Coefficient of base friction = 0.32
3. Passive pressure coefficient = 2.0 (used for sliding calculations)
4. At rest pressure coefficient = 0.45 (used for overturning calculations)

Since for this comparison the soil bearing pressure was the governing factor for foundation design, two foundation bearing pressures were used: one that represented low bearing values (i.e. compacted crush stone/sand) and one that represented high bearing values (i.e. weathered bedrock). A safety factor of 3.0 was assumed for the allowable soil bearing pressures. The following table summarizes the soil bearing criteria and the resulting spread footing width reduction that satisfies design requirements per AASHTO based on LRFD - Strength I design.

Table 9 - Designed Footing Width for Case Study Comparison

Soil Type	Allowable Brg Pressure (Tons/sf)	Strength I Brg Pressure (Tons/sf)	Footing Width, B (ft)	B_ ratio
Low Bearing	2	3	#11 – 8.5 ft	0.76
			# 17 – 6.5 ft	
High Bearing	10	15	#11 – 5.5 ft	0.73
			# 17 – 4.0 ft	

As discussed in previous section, multi-radius arches result in smaller foundations due to a reduced outward thrust that in turn results in smaller foundation bearing pressures. Based on these results, a reduction in foundation width of 0.73 was used. It was also calculated that the governing arch capacity criteria was due to bending and not shear.

An attempt to estimate the cost significance of a multi-radius arch is shown in Table 10.   The incremental cost (Δ _cost) is based on material cost only delivered to the site. Additional construction costs, such as shoring or two step arch filling requirement costs, are not part of this study and have not been considered in the analysis. The base total bridge cost (including demolition, wingwalls, foundation costs, etc.) used for comparison has been assumed at $300/sf for the low end, and $500/sf for the high end, calculated as total construction bridge cost, divided by arch center-to-center span, and divided by total bridge width.

UMaine Composites Center
35 Flagstaff Rd
University of Maine
Orono, ME 04469

16

Telephone: 207-581-2123
FAX: 207-581-2074
composites@umit.maine.edu
www.composites.umaine.edu

Table 10 - Incremental Cost for Multi-radius Arch Bridge Structure

	Δ_arch_ arclength	Δ _arch_ spacing	Δ _Fdn_ Width	Δ _cost_ Low (%)	Δ _cost_ High (%)
FRP Arch	1.07	0.49	NA	+14.17	+23.61
Deck	1.07	NA	NA	+0.16	+0.27
Foundation	NA	NA	0.76	-0.70	-1.17
			Total	**13.63**	**22.72**

It is apparent that the FRP arch cost is the highest factor affecting a multi-radius arch design. Although there are foundation savings, they are not enough to make a multi-arch radius more cost effective than its single radius counterpart. For a 0.3 rise-to-span ratio, increasing the hydraulic opening by 15% will increase the overall bridge cost substantially, estimated between 14 to 23 % increase.

SUMMARY AND CONCLUSION

The design feasibility for multi-radius arches has been studied for three types of bridges with rise to span ratios varying from 0.3 to 0.4. The previously developed code package was expanded to include the non-linear effect of the braid angle within the arches and also to generate multi-radius code to make three radius arch bridges. The modeling was based on a spread footing foundation that closely resembled fixed end conditions.

A case study was used to estimate potential costs incurred in a multi-radius arch structure. The results suggest that although there is a foundation reduction cost due to lower end thrusts, the increase in internal moment in the arches reduce the arch bridge spacing making the overall cost of the bridge more expensive. For the case study, costs incurred for a multi-arch that increased the hydraulic opening by 15 % were estimated between 14 to 23 %.

UMaine Composites Center
35 Flagstaff Rd
University of Maine
Orono, ME 04469

17

Telephone: 207-581-2123
FAX: 207-581-2074
composites@umit.maine.edu
www.composites.umaine.edu

IV. MULTI-RADIUS ARCH TESTING

Two multi-radius arches were manufactured and tested at the Center in January 2015. They were tested with similar rise to span ratios and spans as produced in previous projects for comparisons. In this case though, the arches were manufactured with or near the minimum radius of curvature and with multiple radii of curvature in each arch. Test results were then compared with model predictions.

SPECIMEN DESCRIPTION, TEST SETUP AND INSTRUMENTATION

Two arches were manufactured for testing in December 2014 in the environmentally controlled composites manufacturing lab at the Center. The arches were manufactured using vacuum infusion and materials as described in Dagher et al (2012) but with the geometry shown in Figure 4 and Figure 5. The arches can be seen during manufacturing in Figure 6. Arches were limited from more pronounced multi-radius shapes by the minimum bend radius and desired span of the arches. A 22 foot span with an approximate rise-to-span of 0.30 was desired so that comparisons could be made with similar arches tested with Bannon (2009). A similar rise and span were tested in that test program though with a constant radius arch.
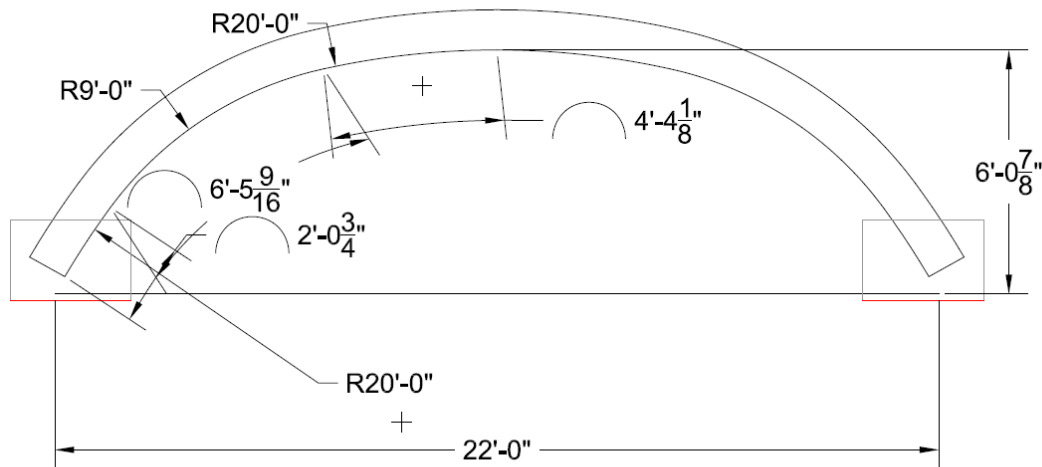

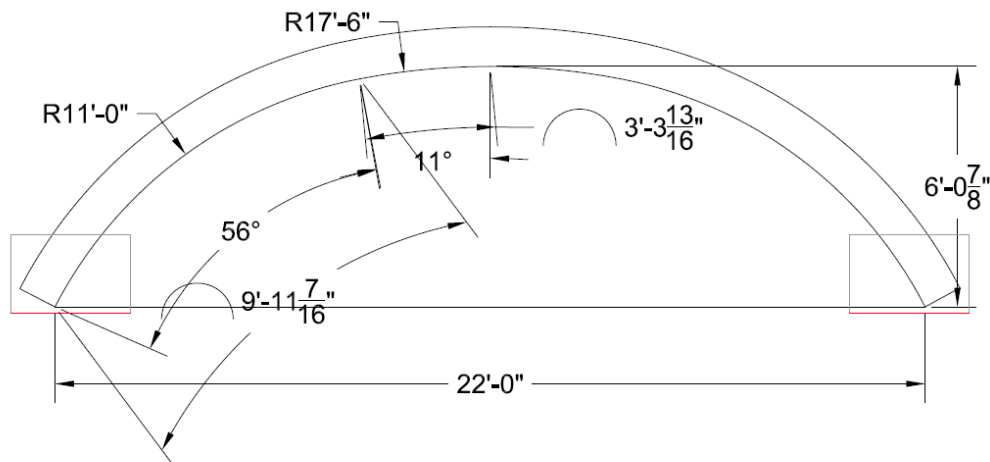Figure 4 - Arch Geometry for Arch 1 (SYM)

Figure 5 - Arch Geometry for Arch 2 (SYM)

UMaine Composites Center
35 Flagstaff Rd
University of Maine
Orono, ME 04469

18

Telephone: 207-581-2123
FAX: 207-581-2074
composites@umit.maine.edu
www.composites.umaine.edu

Figure 6 - Arch on formwork during infusion process

The arches were cast into a reinforced concrete footing and then filled with expansive self-consolidating concrete (6,000 psi unconfined compressive strength) through a 3" diameter hole on top of the crown of the arch. The arch foundations were bolted to steel pin connections that were post tensioned to the reaction floor as seen in Figure 7.

Figure 7 - Arch in fixture with instrumentation

Instrumentation locations are shown in Figure 8. Arches were loaded with a 9" wide and 12" radius of curvature curved load head at a load rate of 0.75 inches per minute at midspan. Stringpots 1 & 5 were used to measure footing rotation. Strain gages are denoted with SG #.

UMaine Composites Center
35 Flagstaff Rd
University of Maine
Orono, ME 04469

19

Telephone: 207-581-2123
FAX: 207-581-2074
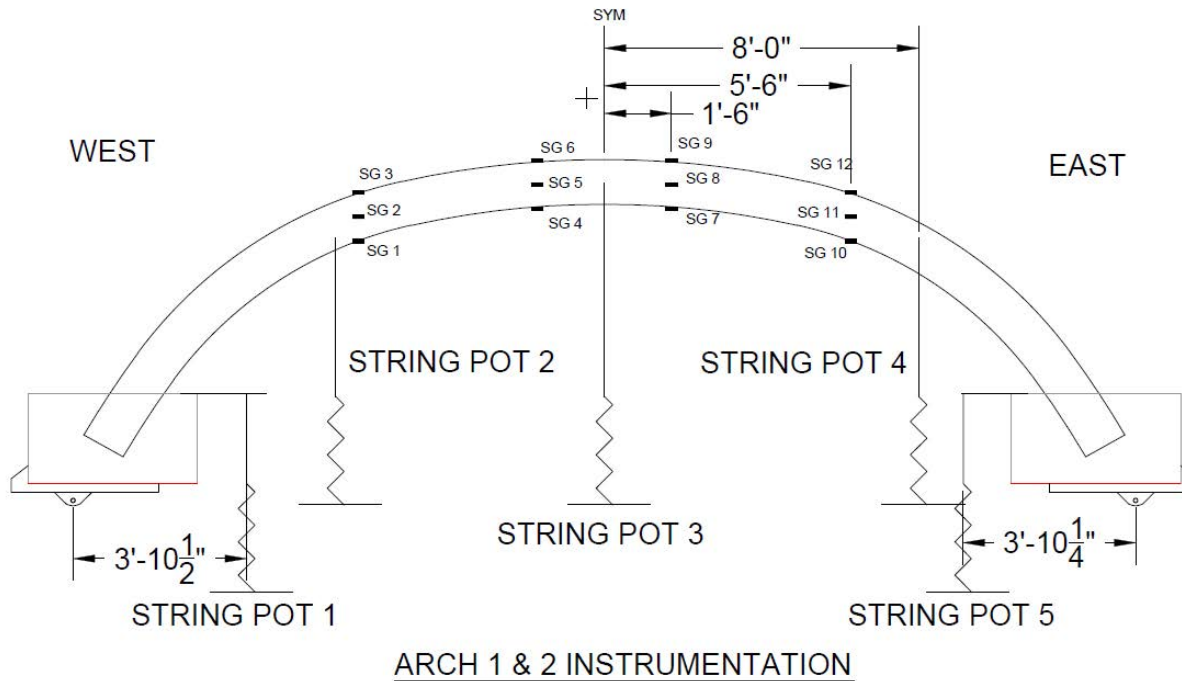composites@umit.maine.edu
www.composites.umaine.edu

Figure 8 – Diagram of sensor locations for Arches 1 & 2

Arches were loaded until failure which corresponded to tensile rupture of the FRP laminate under the crown at the arch where moments were greatest.

RESULTS

Arch 1 and Arch 2 both failed in tensile rupture of the FRP at the crown as seen in Figure 9.

A plot of all strains for Arch 1 is given in Figure 10 where strain is plotted until peak load or until the gage is out of range/failed.

Figure 9 - Tensile rupture of FRP at crown of arch

UMaine Composites Center
35 Flagstaff Rd
University of Maine
Orono, ME 04469

20

Telephone: 207-581-2123
FAX: 207-581-2074
composites@umit.maine.edu
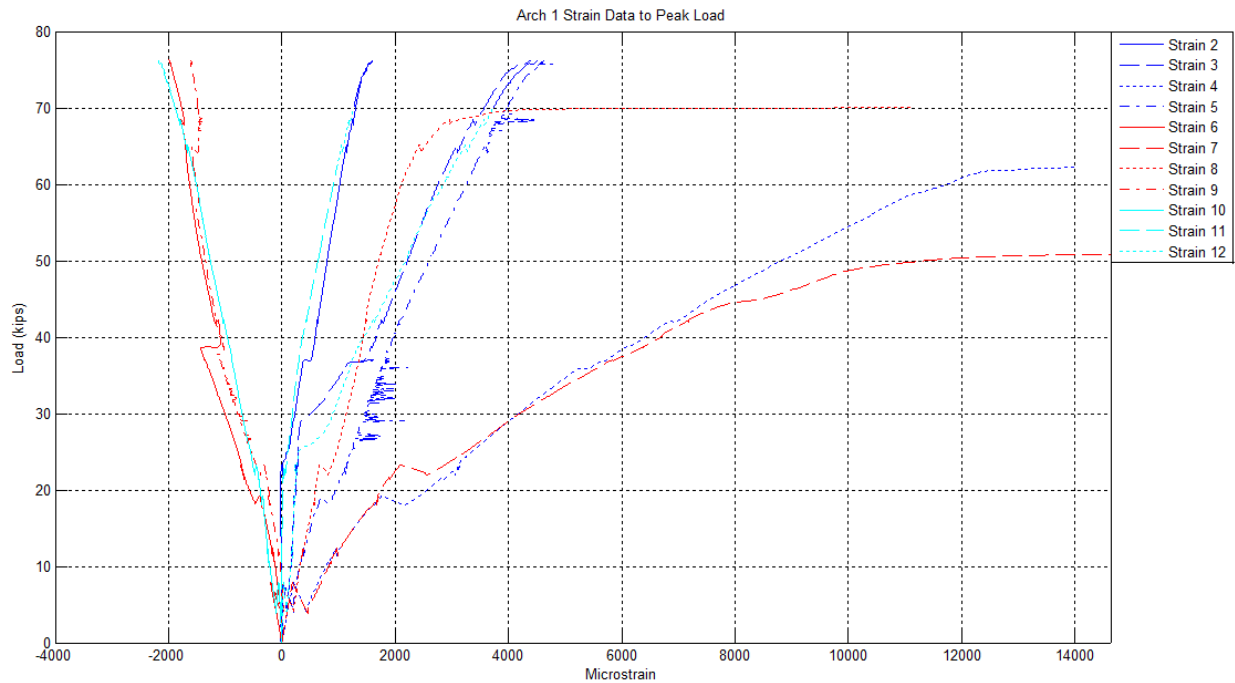www.composites.umaine.edu

Figure 10 – Strain gages 2-12 for Arch 1 test

A peak load of 76,257 pounds was seen for Arch 1. This corresponded to a peak calculated moment of 1,621kip-in using a linear elastic beam element FE model of a pin-pin arch single point load at the midspan node. This model has a relatively course mesh of elements where the concentrated load in the model will over predict real moments. This model matches the analysis performed with the FE model developed for this task. It can then be used to compare the multi-radius arch analysis with the testing.

Deflections of the crown, shoulders and rotational measurements of the string pots can be seen in Figure 11. Shoulder measurements shown are for a single string pot directly below the point of attachment. Some vertical and horizontal movements are seen at this point but not captured with this measurement.

UMaine Composites Center
35 Flagstaff Rd
University of Maine
Orono, ME 04469

21

Telephone: 207-581-2123
FAX: 207-581-2074
composites@umit.maine.edu
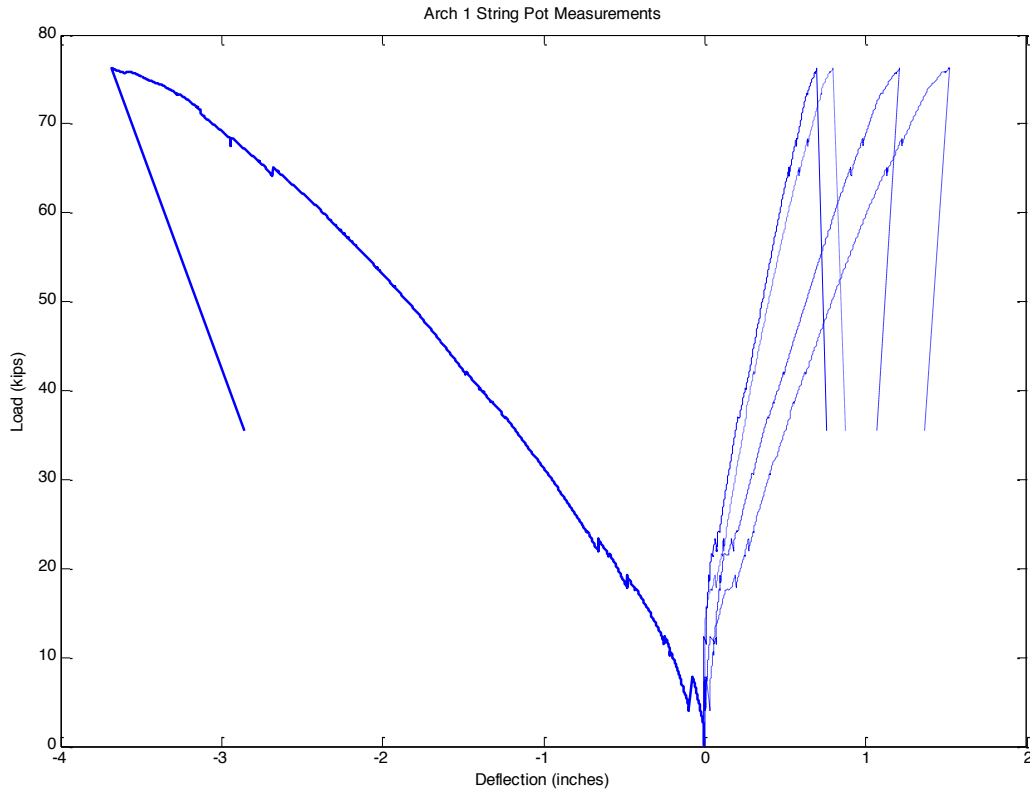www.composites.umaine.edu

Figure 11 – Arch 1 string pot measurements

Arch 2 failed at 75,040 pounds. Strains are plotted against load in Figure 12.   This corresponds to a peak moment of 1,515.7 kip-in using the same analysis as Arch 1.
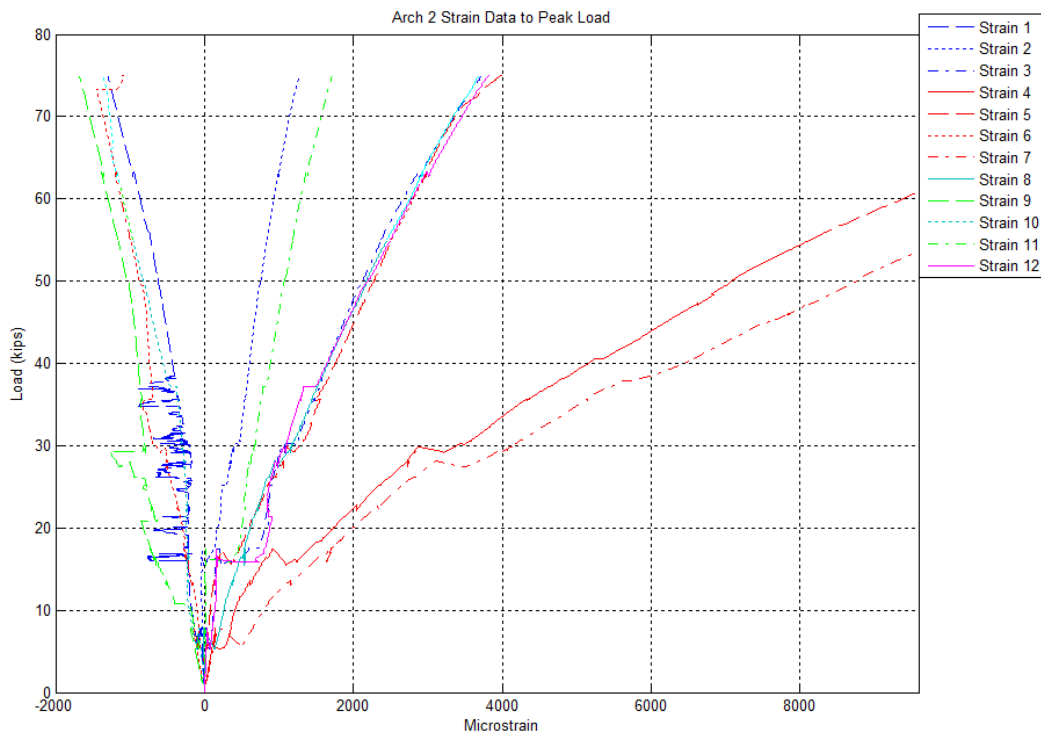

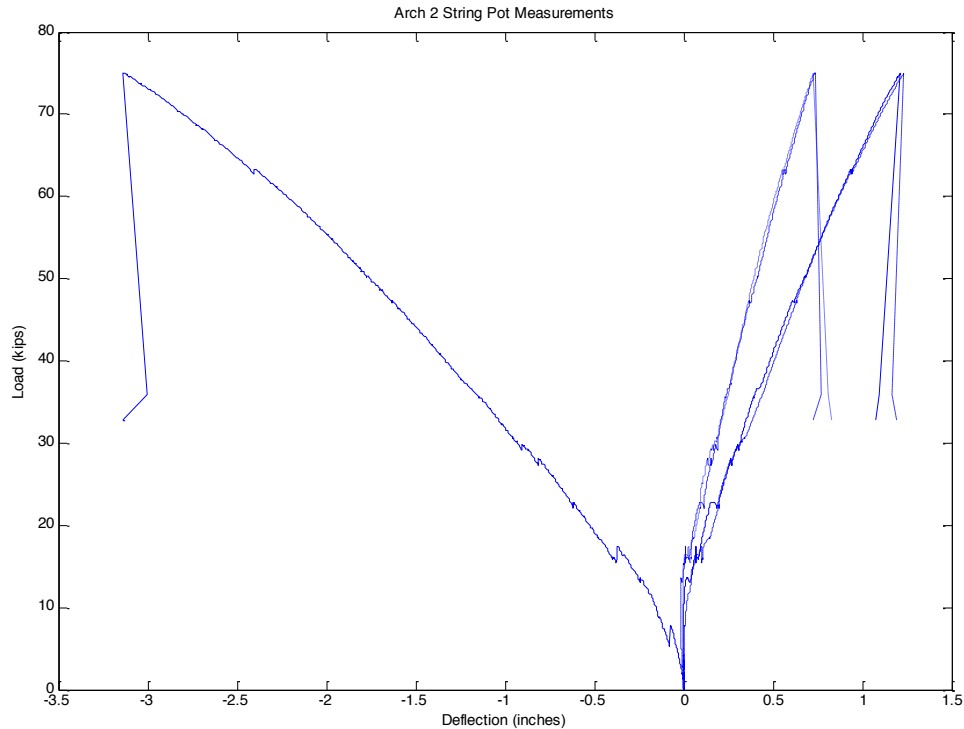Figure 12 – Strain from Arch 2 static test to failure

UMaine Composites Center
35 Flagstaff Rd
University of Maine
Orono, ME 04469

22

Telephone: 207-581-2123
FAX: 207-581-2074
composites@umit.maine.edu
www.composites.umaine.edu

Figure 13 – String pot measurements for Arch 2

COMPARISON WITH MODEL PREDICTIONS

Initial model predictions significantly under-predicted test loads for the two tested arches. As mentioned previously, moment curvature relationships were under predicted in the code developed mainly due to an under prediction of laminate properties from the Classical Lamination Theory analysis with TsaiWu failure theory. Bannon (2009) showed that TsaiWu failure theory under predicted laminate strength but approximately 157% for this laminate. His modeling also took into account stiffened elements for the arch where it was embedded in concrete footings during the test.

Modeling of the arch test was conducted a second time with adjustments for these two factors. Outputs from the micromechanics for strength were increased by a factor of 1.57 and foundations were fixed to account for the stiffened elements near the footings. Table 11 shows a summary of model output and test data. Model outputs now still under predict test results by 13.8% for Arch 1 and 18.1% for Arch 2.

Table 11 - Summary of Model Predictions and Test Data

	First Model Predictions (kips)	Revised Model Predictions (kips)	Test Values (kips)
Arch 1	22.5	65.8	76.3
Arch 2	25.4	61.5	75.0
Bannon (2009) Ave.	N/A	N/A	72.0

UMaine Composites Center
35 Flagstaff Rd
University of Maine
Orono, ME 04469

23

Telephone: 207-581-2123
FAX: 207-581-2074
composites@umit.maine.edu
www.composites.umaine.edu

of Constant Radii Arches			

 More detailed modeling accounting for the stiffened elements with a free rotation condition at the base with appropriate constraints and patch loading at the crown would decrease this error to more reasonable levels as seen in Bannon (2009). The predicted failure loads were also plugged into the linear model discussed in the arch testing. Calculated moments with predicted capacities from the model (1397.7 kip-in & 1151 kip-in for Arch 1 and 2 respectively) agree well with calculated capacities of this cross section from previous testing.

CONCLUSIONS

Arch testing with multi-radius shapes has provided data to refine the code generated in Task 2.1 where larger multi-radius structures can be designed. The code has been shown to be still conservative for this analysis with increases of 57% to the calculated laminate strength outputs. Future use of this code will need analysis comparing TsaiWu failure theory results to baseline laminates, where nominal braid angles through changes in curvature can be analyzed with this code. That factor can be adjusted for each laminate where a multi-radius shape is desired with additional testing.

UMaine Composites Center
35 Flagstaff Rd
University of Maine   24
Orono, ME 04469

Telephone: 207-581-2123
FAX: 207-581-2074
composites@umit.maine.edu
www.composites.umaine.edu

V. ALTERNATIVE MATERIALS FOR EFFICIENT DESIGN, MATERIALS USAGE AND MANUFACTURING

A new arch braid material was also investigated for its ability to easily conform to and be designed for tighter and multiple radii of curvature without wrinkling. The new braid was evaluated for manufacturing efficiency, constructability by manufacturing, and load capacity by testing two full scale arches. They included an initial small, shallow arch and then a larger arch in the shape of previously tested (Bannon 2009) constant radius arches. They were structurally tested for construction loads and long term loading. The new braid is a single heavy layer to replace up to three layers of traditional braided fabrics used in present construction. This single heavy layer has glass fibers nominally in the hoop direction as in previous designs but incorporates additional triaxial carbon tows providing longitudinal tensile reinforcement.

MANUFACTURING TRIALS

The new braid was used in manufacturing trials at the University of Maine Advanced Structures and Composites Center to evaluate how well it can be infused and bent to shape. The infused arch can be seen in Figure 14.

Figure 14- Infused new braid arch

Manufacturing trials did not yield any red flags, and only minor changes to the present manufacturing method were needed. Completions of the manufacturing trials led to structural testing of straight hollow cylinders to evaluate the capacity of the tubes under while being concrete filled. It was expected that this could control many designs of the thin walled concrete filled FRP tubes.

HOLLOW CYLINDER COMPRESSION TESTING

Hollow section compression testing was completed to investigate structural capacity of the hollow section during concrete filling and prior to concrete curing inside the arches.

UMaine Composites Center
35 Flagstaff Rd
University of Maine   25
Orono, ME 04469

Telephone: 207-581-2123
FAX: 207-581-2074
composites@umit.maine.edu
www.composites.umaine.edu

SPECIMENS, TEST SETUP AND INSTRUMENTATION

Thirty (30) inch tall sections of hollow straight tube were manufactured and cut to length similar to Walton (2011). Specimens were tested using end conditions developed in Walton's to achieve results most feasible for even loading during compression testing. One of the specimens during testing can be seen in Figure 15.

Figure 15 - Specimen during hollow compression testing.

Two specimens were tested with holes and three without holes. Specimens with holes depict actual field conditions where the hole is used to fill arches with self-consolidating concrete. The hole here was placed on the side of the section nearest the closest carbon axial. A hole at the

UMaine Composites Center
35 Flagstaff Rd
University of Maine
Orono, ME 04469

26

Telephone: 207-581-2123
FAX: 207-581-2074
composites@umit.maine.edu
www.composites.umaine.edu

crown of the arch would involve cutting the carbon axials and would be expected to greatly reduce structural capacity.

RESULTS

The test results coupled with modeling of structures showed that this new braid is expected to perform as well as the materials that are presently being used for construction of bridges. Though there was not a statistically significant data set, no red flags were noted with data to date.

Table 12 – Results of Axial Compression of Hollow Triaxial Tube

	Peak Load (kips)					Average (kips)	COV	Apparent Reduction
Without Hole	48.63	33.73	31.08	67.40	56.63	47.49	32.3%	19.2%
With Hole	-	-	34.31	42.41	N/A	38.36	14.9%	

Axial stresses from the testing were used to calculate allowable spans of traditional arch bridge designs for hollow arch sections. The construction load analysis would be controlled by the concrete filling loads and other live loads onto the hollow arch. With a rise to span ratio of 0.30 spans would be limited to 45feet here with a hole on one side of the arch, fixed bases and no shoring.

ARCH STRUCTURAL TESTING

Structural arch testing was completed following the compression testing. Two arches were manufactured and tested to failure. A smaller shallow arch was completed first due to material availability. A larger arch was also tested.

TEST SPECIMENS, SETUP AND INSTRUMENTATION

Setup of the test can be seen with instrumentation installation in Figure 16. Strain, deflections, and load were collected during each test.

UMaine Composites Center
35 Flagstaff Rd
University of Maine
Orono, ME 04469

27

Telephone: 207-581-2123
FAX: 207-581-2074
composites@umit.maine.edu
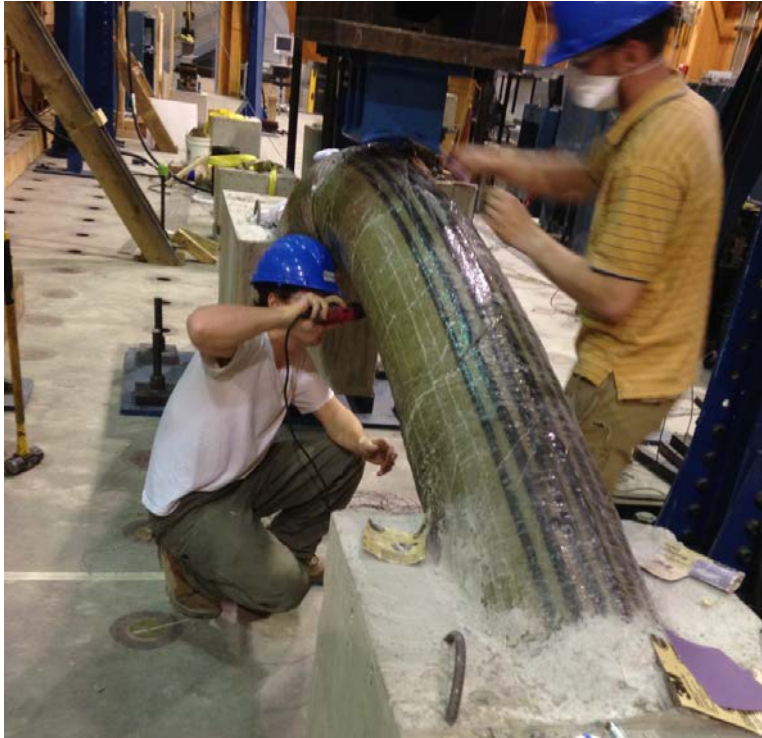www.composites.umaine.edu

Figure 16 - Arch test setup

The ends of each arch were cast into 2 foot by 2 foot by 4 foot reinforced concrete footings. The footings were bolted to rocker bearings and post-tensioned to the structural testing floor at the Center. The shallow arch had a clear span of approximately 8 feet with 5:1 span to rise ratio.

The larger arch had a span of 22feet with a radius of curvature of 13feet as seen in previous testing (Bannon 2009). This arch was loaded with a point load at the crown at 0.50 inches per minute. This arch was filled with concrete through a hole in the side of the arch at the crown which is different from every other arch and did cause problems. Voids needed to be grouted around the crown where concrete setup prior to completely filling the arch. Grouting was not completely successful as noticed during and after the test.

RESULTS

A peak load close to 130 kips was seen during the structural test. Support underdesign, though, forced the test to be stopped prior to full failure of the arch as seen in Figure 17. Glass fiber de-laminations were seen with likely fiber breakage near the crown of the arch.

UMaine Composites Center
35 Flagstaff Rd
University of Maine
Orono, ME 04469

28

Telephone: 207-581-2123
FAX: 207-581-2074
composites@umit.maine.edu
www.composites.umaine.edu

Figure 17 – Shallow Arch post test

Figure 18 - Arch tensile failure at midspan of shallow arch

UMaine Composites Center
35 Flagstaff Rd
University of Maine
Orono, ME 04469

29

Telephone: 207-581-2123
FAX: 207-581-2074
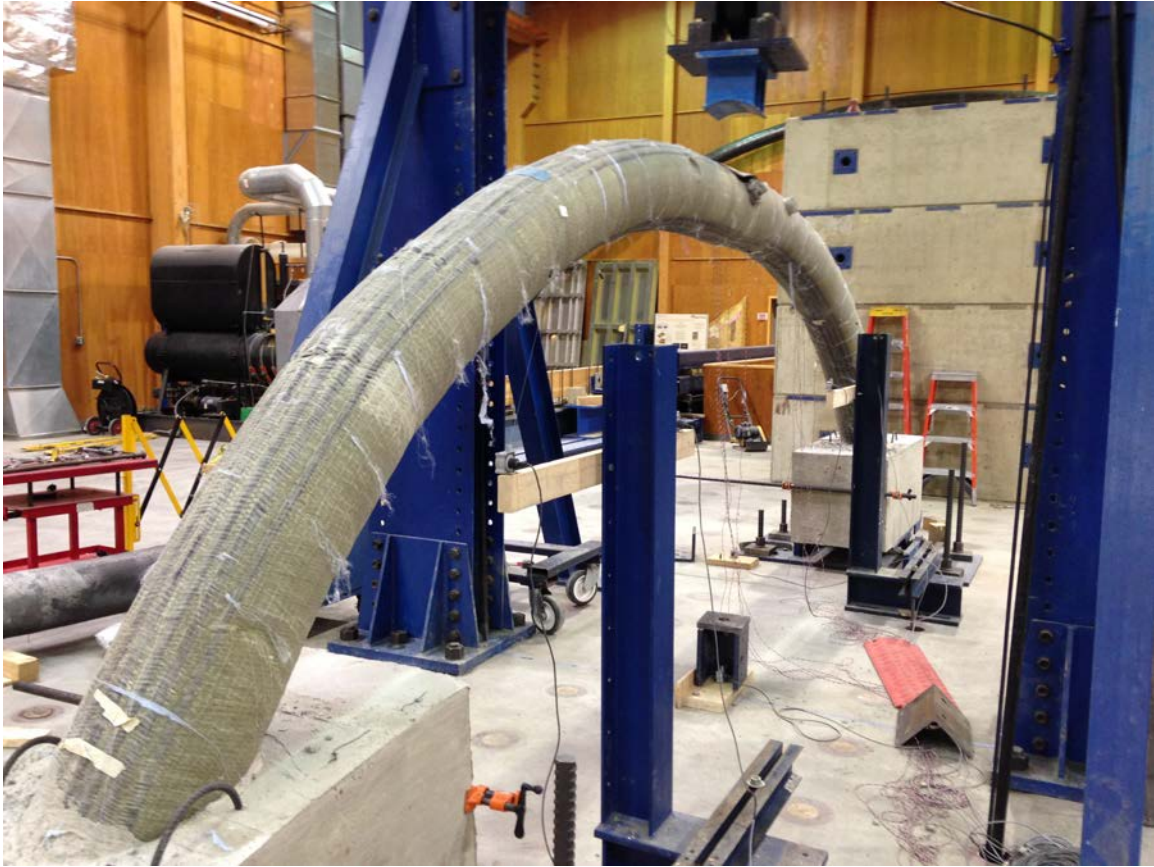composites@umit.maine.edu
www.composites.umaine.edu

Figure 19 - Failed tall arch

A calculated peak bending moment of approximately 881 kip-inches was achieved and it is lower than tests with materials used to date (approximately 1400kip-inches).

Figure 20 shows the strain data from the arch test. Gages where peak strain are cut off where they went out of range or failed at approximately 50 kips.

UMaine Composites Center
35 Flagstaff Rd
University of Maine   30
Orono, ME 04469

Telephone: 207-581-2123
FAX: 207-581-2074
composites@umit.maine.edu
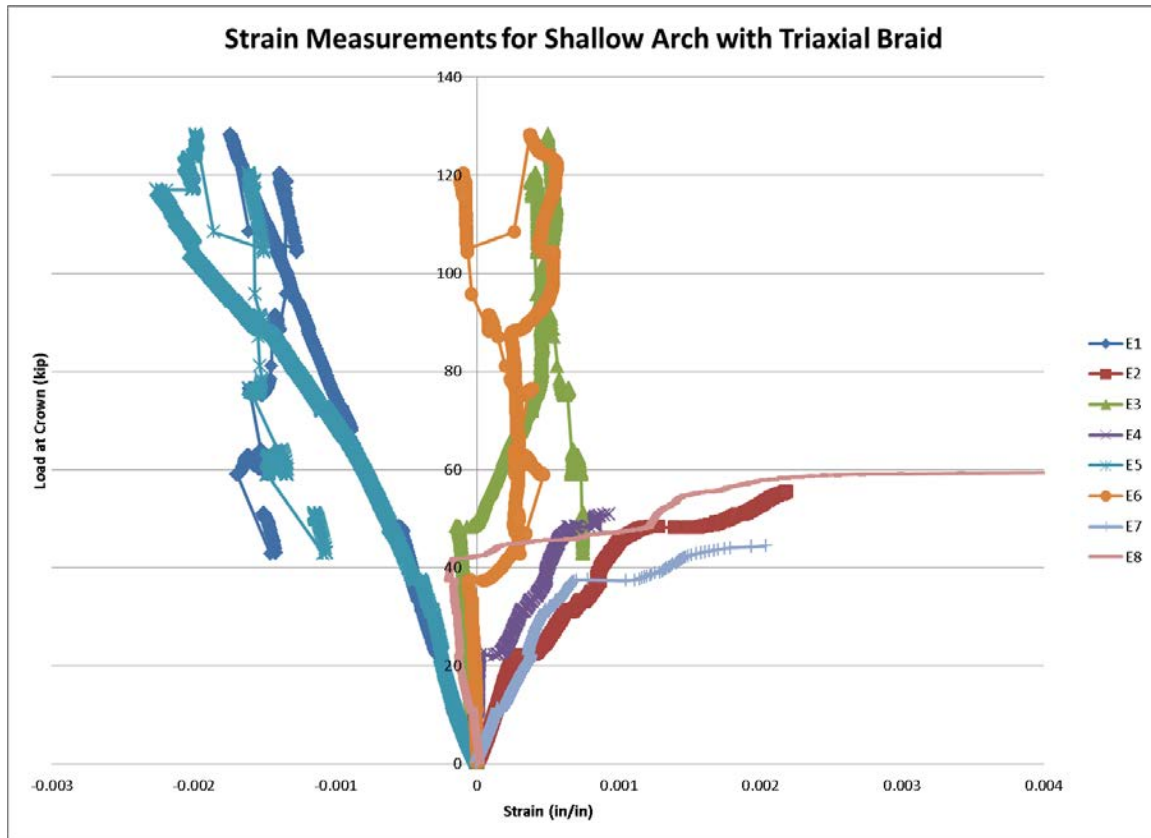www.composites.umaine.edu

Figure 20 - Strain versus load plot for shallow arch

The second tall arch reached a peak load of 53,209 pounds. Using a similar linearly elastic pin-pin arch with a course beam element model a peak moment of 886 kip-in calculated with the peak load from the test. The plot of midspan vertical deflection can be seen in Figure 21. Strain gages near midspan failed between 10 kips and 20 kips and are not presented. Strains at the shoulder are presented in Figure 22. Ultimate failure appeared to occur at the crown and shoulder where discoloration is seen in the glass fibers. Carbon axial fibers do not appear ruptured though. Discoloration is seen along the length of the carbon axials though (Figure 24). In this figure the left hand side of the photo, whitening is seen around the carbon axial tows.
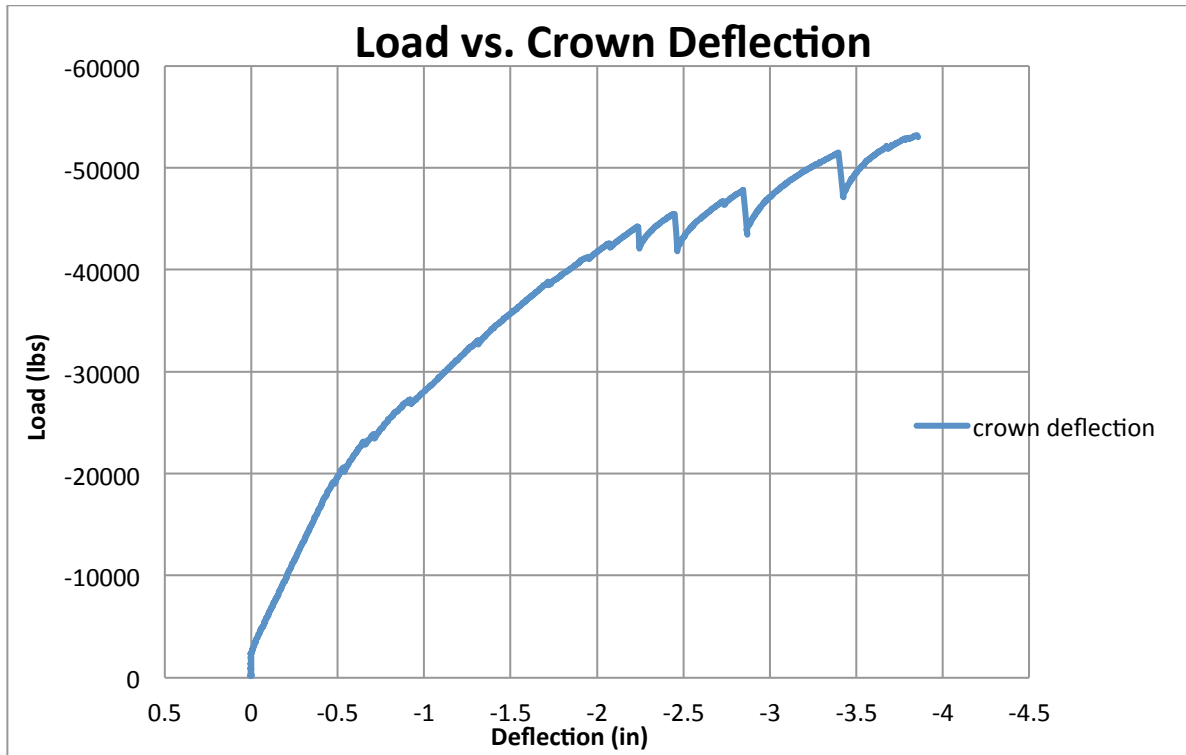
UMaine Composites Center
35 Flagstaff Rd
University of Maine
Orono, ME 04469

31

Telephone: 207-581-2123
FAX: 207-581-2074
composites@umit.maine.edu
www.composites.umaine.edu

Figure 21 - Plot of load and deflection at crown of tall arch

Figure 22 - Strains at shoulders of arch

UMaine Composites Center
35 Flagstaff Rd
University of Maine
Orono, ME 04469

32

Telephone: 207-581-2123
FAX: 207-581-2074
composites@umit.maine.edu
www.composites.umaine.edu
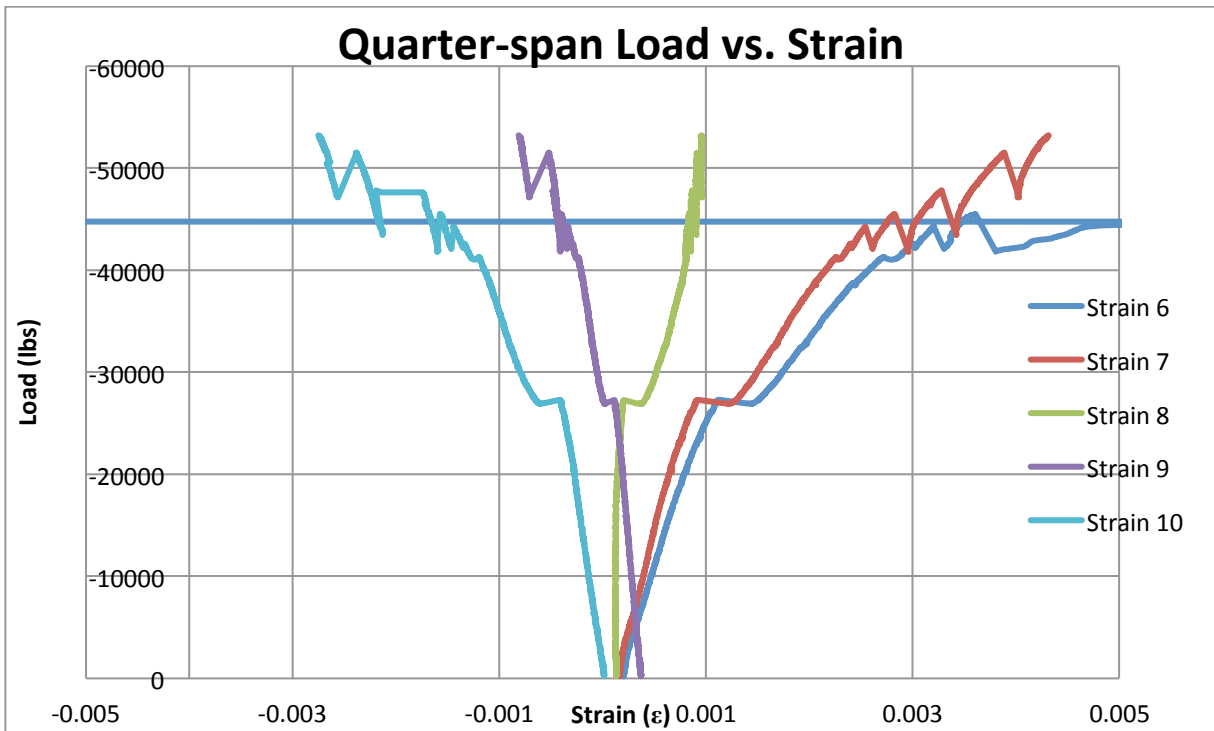
Figure 23 – Top of arch near midspan due to void in concrete

Figure 24 - Underside of midspan of arch after failure (discoloration seen on left)

DISCUSSION AND CONCLUSIONS

Neither the shallow or tall arch reached predicted capacities as predicted for tensile rupture of the carbon axials at the crown. The footings and supports failure was the ultimate stopping point for the shallow arch where the arch was behaving more as a tall cambered beam then an arch.

The grouting of voids at the crown was not completely successful. The void forced the load head to move downward on the arch and rotate where side load was also being put on the arch. This could have partially contributed to the lower peak load than predicted. Another probable cause could be partial disbonding of the carbon axial tows as indicated by the areas of delamination or whitening around the tows visible in Figure 24.

Results for both arches are applicable for radii of curvature tested here or greater as tigher radii arches will see greater tear out stresses from the carbon fiber axials. This forces has not been investigated here.

The arch testing served as a successful screening study for alternative materials that will allow for more efficient designs and with completed studies allow for easier manufacturing and design of arches with single or multiple radii.

UMaine Composites Center
35 Flagstaff Rd
University of Maine
Orono, ME 04469

33

Telephone: 207-581-2123
FAX: 207-581-2074
composites@umit.maine.edu
www.composites.umaine.edu

VI. REFERENCES

Bannon, D.J. (May 2009). *Characterization of Concrete-Filled Fiber Reinforced Polymer Arch Members*, M.S. Thesis, The University of Maine, Orono, ME.

Clapp, J.D. and Davids, W.G. (2011). *Simplified Modeling to Assess Soil-Structure Interaction*, AEWC Report No. 11-30.

Clapp, J.D. and Davids, W.G. (2011). *Development of Enhanced Software for Analysis of soil-Structure Interaction and Foundation Design*, AEWC Report No. 12-25.1049.

Dagher, Habib, et al. *Concrete-Filled Tubular FRP Arches for Rapidly Erected Bridges*. TRP 91st Annual Meeting. January 22-26, 2012. Washington D.C.

Das, B. M. (2004). *Principles of Foundation Engineering* (5th ed.). Brooks/Cole Thomson Learning, Inc. USA.

MathWorks (2009). *Programming Fundamentals, MATLAB Version 7.9 (R2009b)*, The MathWorks, Inc. Natick, MA.

Walton, H.(2011) *Response of FRP Arches to Concrete Filling Loads*. Master's Thesis, Dept. of Civil and Environmental Engineering, University of Maine.

UMaine Composites Center
35 Flagstaff Rd
University of Maine
Orono, ME 04469

34

Telephone: 207-581-2123
FAX: 207-581-2074
composites@umit.maine.edu
www.composites.umaine.edu